Desalination 488 (2020) 114383

Contents lists available at ScienceDirect

Desalination

journal homepage: www.elsevier.com/locate/desal

Energy consumption in membrane capacitive deionization and comparison with reverse osmosis

S. Porada[a,b], Li Zhang[a], J.E. Dykstra[c,*]

[a] Wetsus, European Centre of Excellence for Sustainable Water Technology, Oostergoweg 9, 8911 MA Leeuwarden, The Netherlands
[b] Soft Matter, Fluidics and Interfaces Group, Faculty of Science and Technology, University of Twente, Drienerlolaan 5, 7522 NB Enschede, The Netherlands
[c] Environmental Technology, Wageningen University, Bornse Weilanden 9, 6708 WG Wageningen, The Netherlands

A B S T R A C T

Membrane capacitive deionization (MCDI) is a technique for water desalination by adsorbing ions in charged porous electrodes. In the present experimental and theoretical study, we analyze the performance, in terms of energy consumption, salt rejection and water recovery, of MCDI operated in intermittent flow mode. With this mode, the water recovery of MCDI is increased by reducing the water flow ratio during regeneration. Both experimental and theoretical results show that high values for water recovery and salt rejection can be achieved with a lab-scale MCDI system for feed water with a salinity of 40 mM. Importantly, we find that the energy requirement of MCDI is a factor of 2.0–2.5 higher than of RO. For RO, the energy requirements were calculated with a system-scale model developed by Qin et al. [1]. Furthermore, we show that, based on our theoretical predictions, improved MCDI can reach high salt rejection and water recovery, without an additional energy penalty. In these conditions, the energy consumption of MCDI is lower than of RO. In the present work, we present new insights for a fair performance comparison of MCDI and RO.

1. Introduction

"*Capacitive deionization* (*CDI*), *during which salt is removed via an electrochemical method, has emerged in an effort to tackle the limitations of the complex infrastructure and high cost of other well-developed desalination technologies* (*e.g.*, *reverse osmosis and nanofiltration*)" [2]. By applying a voltage over two porous electrodes, often made from activated carbon, ions are removed from the feed water and are adsorbed into the micropores of the electrodes, resulting in a desalinated water stream. After the electrodes are saturated with salt ions, the electrodes are regenerated and the adsorbed ions are released from the electrodes and are flushed out, resulting in a concentrated effluent solution. Since the early 2000s, CDI gained much scientific and commercial interest. Scientists focused on the development of innovative cell designs [3,4] and new electrode materials [2,5–10]. One of these developments was the inclusion of ion-exchange membranes in the cell, which resulted in an increased salt adsorption performance [11,12]. We refer to this cell design as Membrane Capacitive Deionization (MCDI). Furthermore, specific applications were explored for CDI, including ion-selective removal [13–23]. Lastly, several studies have been performed to identify resistances in CDI and MCDI devices [24,25], to study the energy efficiency of (M)CDI [26,27] and to compare the energy consumption between two different operational modes: constant voltage and constant current [28,29].

In order to study the energy efficiency of CDI, and to calculate energy losses due to resistances, several experimental and theoretical studies have been conducted. Theoretical (M)CDI models describe various aspects, such as the adsorption of ions in the porous (carbon) electrodes and the transport of ions in the ion exchange membranes and in the flow channel [30–32]. To calculate the adsorption of ions in the micropores of (porous) electrodes, the modified Donnan model, the improved modified Donnan model and the amphoteric Donnan model are often used [22,33–36]. These models, which describe both physical and chemical phenomena, have been validated against experimental data, and have shown to accurately predict the salt adsorption performance in equilibrium conditions [6,22,23,34,37]. To describe the dynamics of desalination with porous (carbon) electrodes, the Donnan models can be coupled with ion transport theory. These dynamic models have also been extensively validated.

A highly debated topic in the field of CDI is whether CDI is more energy-efficient than state-of-the-art desalination technologies such as reverse osmosis (RO) [38]. For example, a study by Zhao et al. [39] states that CDI is, compared to RO, more energy-efficient for brackish water desalination. However, in other studies it is argued that a comparison of desalination technologies in terms of energy performance is very difficult, and that the result of such a comparison is dependent on the desalination objective, which is defined by the water recovery and the desalination rate [5,26] [40]. In Ref. [28] we presented a robust methodology to compare two operational modes in CDI and we argued that a fair comparison must meet two conditions: I) the desalination

* Corresponding author.
E-mail address: jouke.dykstra@wur.nl (J.E. Dykstra).

https://doi.org/10.1016/j.desal.2020.114383
Received 28 November 2019; Received in revised form 15 January 2020; Accepted 14 February 2020
Available online 18 May 2020

objective, which is dictated by the water recovery, the desalination rate and the feed water conditions, must be the same in both modes, and II) the modes must be operated under optimized conditions. In other words, for a given desalination objective, the operational conditions of both modes must result in the lowest energy consumption. This second condition is hard to meet, as many experiments must be performed to identify which operational conditions result in a desalination performance with the lowest energy consumption. Alternatively, one can perform many theoretical calculations with an experimentally validated model. In order to compare two desalination technologies, such as RO and CDI, we argue that conditions I) and II) apply as well.

A fair comparison between the energy efficiency of desalination technologies is extremely challenging, and only a few papers have been published to compare the performance of CDI with other desalination technologies, such as RO and ED [39]. A recent paper by Qin et al. compared the energy efficiency of CDI with RO using system-scale models [1]. The authors found that RO is significantly more energy efficient than CDI, especially when targeting feed streams at higher salinity, and with high values for salt rejection and water recovery. For example, the desalination of brackish water with a salt concentration of 2 g/L, achieving 80% water recovery and 80% salt rejection, and with an average desalinated water flux of 10 L/m^2/h, requires with CDI a specific energy consumption of approximately 2.5 kWh/m^3 (without energy recovery), which is, according to Ref. [1], about 35 times higher than the energy consumption of RO (0.073 kWh/m^3). This study also concluded that current efforts to improve electrode materials in CDI can only marginally reduce the energy consumption. After publication, several scientists commented on the paper. Ref. [41] argues that based on the shortcomings of CDI technology unveiled by Ref. [1], researchers and funding agencies should better examine the commercial viability of any new desalination technology. Counterfacts are posed in a comment [42] in which the authors report higher thermodynamic efficiency values for a conventional CDI system than reported in Ref. [1], and the authors foresee further improvements for CDI-systems with optimized flow efficiency, and with lower resistances.

Other criticism voiced in Ref. [42] is that in the study in Ref. [1] an uncommon theoretical approach was used to calculate the energy consumption for CDI. Qin et al. [1] base their findings on a simplified Randles Circuit model, which predicted unphysical trends as argued in Ref. [42]. The model used in Ref. [1] was not extensively validated with experimental data. Besides, the energy efficiency was only studied for a limited number of operational modes, and this approach resulted in non-optimized (high) values for energy consumption of CDI. Lastly, the authors used a simplified RO modeling approach, and they used an uncommon definition of the salt rejection in the RO model, which is different from the definition used for CDI, as we will discuss in more detail below.

In the present work, we report novel results of MCDI operated in the so-called intermittent flow mode, which was introduced in Ref. [43]. The intermittent flow mode consists of three sequential steps: desalination, regeneration and flush-out. During desalination, when feed water flows through the cell, a constant current is applied, and ions are adsorbed from the feed water into the porous electrodes. During regeneration, the current is reversed and salt is released from the electrodes, while the feed water flow is paused. Therefore, the salt concentration in the flow channel increases to high values. After regeneration, the flow is restarted, and the concentrated salt solution in the flow channel is removed from the cell. We show, experimentally and theoretically, that this intermittent flow operation results in a high water recovery and more optimized energy consumption, much higher than obtained in conventional operation of MCDI cells. Furthermore, we compare our data with the energy consumption of RO calculated by Qin et al. [1]. To that end, we corrected their RO results by using the same general definition of salt rejection, such that the same metrics are used when comparing RO and CDI, something that was not done in Ref. [1]. We find that the energy consumption of RO and CDI is comparable, and that the differences are much lower than those calculated by Qin et al. [1].

Table 1
Operational parameters, electrode, membrane and flow channel dimensions, and settings for theoretical calculations.

Operational Unit		Parameters Fig. 3		Parameters Fig. 4	
		$MCDI_1$	$MCDI_2$	bar(C) MCDI	bar(E) MCDI
I (A/m^2)	Current density	18.5	22.0	20.1	25.3
t (s)	Duration of the desalination (des) step	400	340	340	1020
	regeneration (reg) step	370	310	310	990
	flush-out (flo) step	30	30	30	30
Φ (mL/min)	Flow rate through each cell during the desalination (des) step	1.25	1.25	1.25	1.25
	regeneration (reg) step	0	0	0	0
	flush-out (flo) step	**	**	3.0	1.65
Electrode					
A_{cell} (cm^2)	Electrode geometric surface area	33.75		33.75	33.75
L_{elec} (μm)	Electrode thickness	250		250	350
EER (Ω m^2)	External electronic resistance	15		15	7.5
C_S (F/mL)	Stern capacitance in the zero-charge limit	170		170	340
E (kT mol m^{-3})	Micropore ion-correlation energy	100		100	100
α (F m^3 mol^{-2})	Charge dependence of Stern capacitance	20		20	20
p_{mA}	Macroporosity	0.5		0.5	0.5
p_{meso}	Mesoporosity	0.05		0.05	0.05
p_{mi}	Microporosity	0.34		0.34	0/34
Membrane					
L_{mem}(μm)	Membrane thickness	160		160	250
ωX (M)	Charge density of the anion / cation exchange membrane	+5/-5		+5/-5	+10/-10
p_{mem}	Membrane porosity	0.3		0.3	
Flow channel and other					
L_{sp}(μm)	Flow channel thickness	100		100	100
p_{sp}	Flow channel porosity	0.5		0.5	0.9
N_{cells}	Number of cells in the CDI stack	10		10	10
V_{dead} (mL)	Dead volume per cell	0.45		0.45	0.15
D_{KCl} (m^2/s)	Average diffusion coefficient of K^+ and Cl^- (in free solution)	2.03*10^{-9}		2.03*10^{-9}	2.03*10^{-9}

**The flow rate during flush-out is different for each experiment.

2. Theory

In the present work, we employ the MCDI model as presented in Ref. [25] to describe transport of ions in the flow channel, membranes and porous electrodes, and to describe the adsorption of ions in electrical double layers (EDLs) formed in the micropores of the porous electrodes. To model adsorption of ions, this MCDI model employs the improved modified-Donnan (i-mD) model, which describes ion adsorption in the EDLs as function of a Donnan potential and an attraction term, μ. The model has been validated with experimental work and has been used in numerous scientific papers to describe the performance of CDI and MCDI cells [25,28]. Later, a physically and chemically more correct version of the i-mD model has been introduced, the amphoteric Donnan

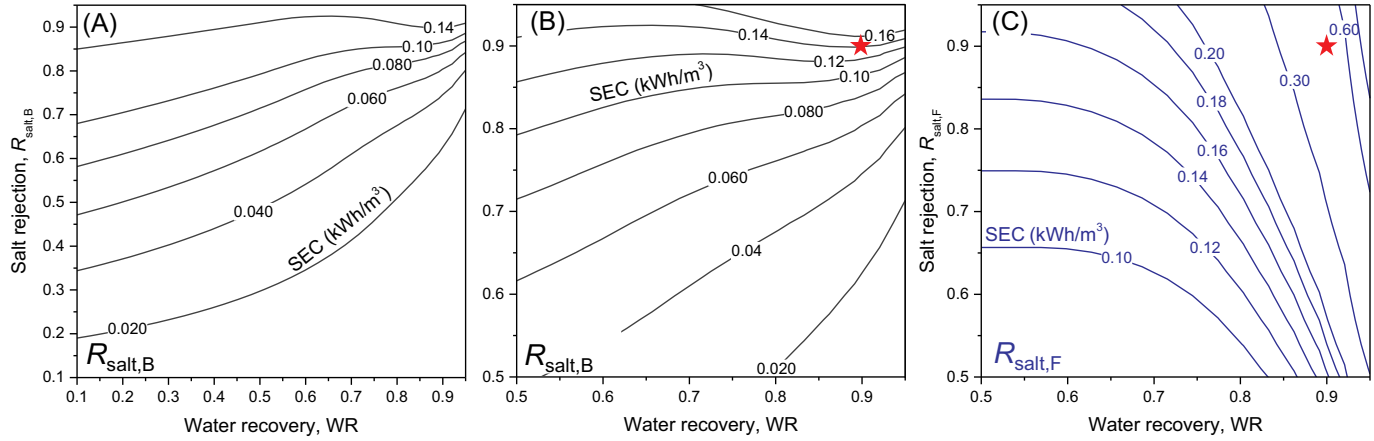

Fig. 1. (A) A reproduction of the calculated specific energy consumption from Qin et al. [1] for RO (their Fig. 8B) as function of water recovery (WR) and salt rejection calculated using brine water concentration ($R_{salt,B}$) (Eq. (1)). (B) The same plot as in Fig. 1A with WR > 50% and R_{salt} > 50%. (C) RO specific energy consumption as function of WR and the salt rejection calculated using feed water concentration ($R_{salt,F}$) (Eq. (2)). Feed salinity 2 g/L, and membrane flux 10 L m^{-2} h^{-1}. The red star indicates a desalination with WR = 0.9 and R_{salt} = 0.9, and if R_{salt} is calculated based on the brine water concentration, SEC = ~0.14 kWh/m^3 (Fig. 1B), and based on the feed water concentration SEC = ~0.45 kWh/m^3 (Fig. 1C), which is a difference of around a factor of 3.5.

(amph-D) model [36,37]. Although the amph-D model is more realistic, we show in S.I. Section 1 in Ref. [28] that, when we stay in a limited salt concentration range, the predicted desalination performance and voltages by the i-mD and amph-D models are very comparable. Compared to the MCDI model in Ref. [25], we make one simplification: we model the flow channel as one single perfectly mixed compartment, i.e., we do not consider concentration gradients across the channel. Furthermore, we include a mass balance to evaluate the effluent concentration of the MCDI cell based on the flow-rate through the MCDI stack and a small dead volume after the stack. To that end, we include Eq. (13) reported in Ref. [44]. Because of the presence of a small dead volume, the effluent concentration of the MCDI stack is different from the concentration in the spacer channel. Consequently, during regeneration the salt concentration increases in the spacer channel to high values, even above the salt concentration in the electrodes, while the effluent concentration does not increase (the flow rate during regeneration is 0 mL/min). During flush-out, the effluent concentration strongly increases, while the salt concentration in the spacer channel decreases. We report the parameter values used for our calculations in Table 1. All other modeling details are found in Refs. [25, 32].

3. Materials and methods

MCDI experiments were performed using a flow stack which contained ten parallel flow cells. Each cell consisted of two porous carbon electrodes (Materials & methods, PACMM™ 203, Irvine, CA, δ_e ~250 μm, dry weight of two electrodes is m_e = 1.1 g per cell) and a porous polymeric spacer (δ_{sp} ~100 μm), which serves as a flow channel. In each cell, an anion exchange membrane (Neosepta AMX, Japan) was placed between the positively polarized electrode and the flow channel, and a cation exchange membrane (Neosepta CMX, Japan) between the negatively polarized electrode and the flow channel. To connect the porous electrodes with the electrical circuit, graphite current collectors (thickness δ ~250 μm) were used. The system was operated in single-pass mode [13] and an aqueous solution with a feed composition of 40 mM NaCl was pumped through the flow channels. The outlet conductivity was continuously monitored and the effluent salt concentration was calculated using a calibration curve.

In the present work, we use a novel operational mode to charge and discharge the cell [43]. With the aid of this operational mode, we aim to increase the water recovery, the salt rejection, and to reduce energy losses due to resistances, compared to more common studies in CDI where water recovery is around 50%, and salt rejection generally not beyond 50%, but often much lower (i.e., less salt removal). Our results therefore have relevance also by themselves, in addition to the relevant comparison with RO operation. The new operational mode consists of three sequential steps: desalination, regeneration, and flush-out. A description of each of these steps is as follows:

- During desalination, we apply a constant current density of I_{ch} for the duration of the step, t_{des}, and we operate the cell with a constant flow rate of Φ_{des}.
- During regeneration, the current is reversed and the value is slightly higher compared to the desalination step, such that the total charge transferred is the same for the charging and discharge step, and ensuring that the duration of the regeneration plus flush-out step together, is equal to the duration of the desalination step, thus $t_{des} = t_{reg} + t_{flo}$. In this step we reduce the flow rate to zero, $\Phi_{reg} = 0$, and therefore all the salt stored in the porous electrodes and is released into the flow channel, stays there, resulting in a strong increase of the salt concentration in the channel.
- During flush-out, no electrical current runs between the electrodes, and we increase the flowrate to Φ_{flo}.

During desalination and regeneration, the maximum voltage (or upper voltage) for charging and the minimum voltage (or lower voltage) for discharge were not controlled, but the cell voltage did not exceed the voltage window between −1.0 and +1.4 V. We calculated the energy consumption, water recovery, and salt rejection of desalination according to the definitions reported in Ref. [40]. The thermodynamic efficiency of desalination was calculated according to Ref. [26].

4. Results and discussion

4.1. Different salt rejection definition used in RO and CDI in Qin et al. [1]

In order to compare in a fair manner energy consumption of MCDI in this study with the values for energy consumption of MCDI and RO reported by Qin et al., we present a revised version of Fig. 8B from Ref. [1]. This step is necessary because Qin et al. used an uncommon definition of the salt rejection in the RO model to describe the system-scale salt rejection, which is not the same as the one commonly used to describe desalination processes (namely the definition they used to discuss their results for CDI) [45–47]. The use of two different salt rejection definitions renders impossible a fair comparison of the energy

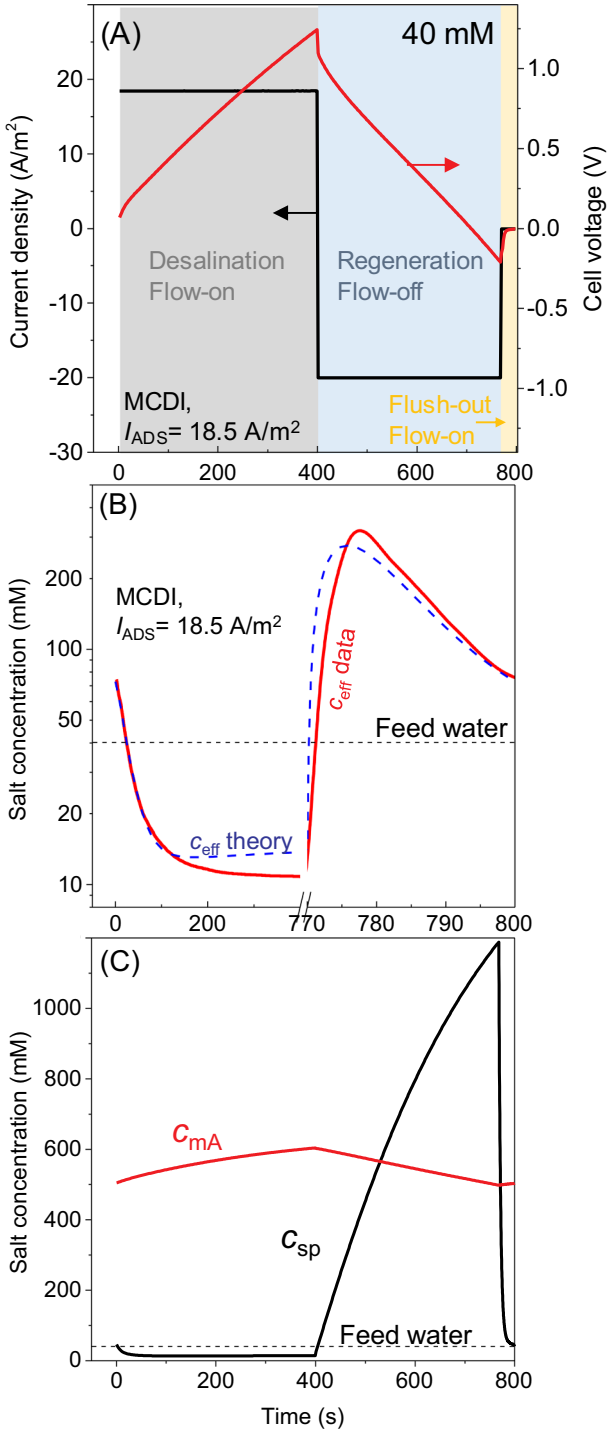

Fig. 2. MCDI operation at high water recovery and salt rejection by operation with intermittent flow. (A) Experimental results for current density and cell voltage; (B) Experimental (red solid line) and theoretical (blue dashed line) results for effluent salt concentration. (C) Theoretical salt concentration in the flow channel and in the macropores as function of time. (The feed water concentration was 40 mM, the flush ratio was 8.9 (see Eq. (4) for the definition of the flush ratio), and the charging current density was 18.5 A/m^2).

consumption as presented in Fig. 8 in Ref. [1], especially at high water recovery.

In Ref. [1] the RO salt rejection is defined as

$$R_{salt,B} = 1 - \frac{c_P}{c_B} \quad (1)$$

where c_P is the effluent salt concentration and c_B the brine salt concentration. In contrast, Ref. [1] defines the salt rejection for CDI as

$$R_{salt,F} = 1 - \frac{c_P}{c_F} \quad (2)$$

where c_P is the effluent salt concentration and c_F is the feed salt concentration. The definition in Eq. (2) is the common definition for salt rejection [45,47].

In Ref. [1], Eq. (1) is used to calculate the salt rejection for RO, and Eq. (2) is used to calculate salt rejection for CDI, while the results are reported with the same symbol, R_j, and results are presented in two panels next to each other in Figs. 6, 7 and 8. We argue that this approach was erroneous, and the authors did not succeed in presenting a fair comparison between RO and CDI performance.

Using a mass balance for salt and for water, the two salt rejections can be related by

$$R_{salt,F} = 1 - \frac{1 - R_{salt,B}}{1 - WR \cdot R_{salt,B}} \quad (3)$$

where $R_{salt,F}$ is the salt rejection given in Eq. (2), $R_{salt,B}$ is the salt rejection given in Eq. (1) and WR is the water recovery. Fig. 8B from Ref. [1] was recalculated and the results are presented in Fig. 1A. An expanded view, focusing on the region of WR > 0.5 and R_{salt} > 0.5 is shown as Fig. 1B. A revised version of the exact same calculations, but now with the salt rejection $R_{salt,F}$ as the operational parameter on the y-axis (instead of $R_{salt,B}$ as in panel A and B), defined according to Eq. (2), is presented in Fig. 1C.

We used the same RO model as in Ref. [1] and could reproduce Fig. 8B (from Ref. [1]), which is Fig. 1A as presented in this paper. Fig. 1A presents lines of constant specific energy consumption (SEC, in kWh/m^3 of diluate produced) in a graph with water recovery, WR, on the x-axis, and salt rejection, $R_{salt,B}$, on the y-axis as defined by Eq. (1). Fig. 1B shows the same plot but focuses on the most relevant upper-right quadrant where WR > 50% and salt rejection > 50%. These two graphs have many peculiar features, such as for constant salt rejection and increasing WR this can result in *SEC being lowered*. Another peculiar feature is that at certain values of salt rejection, for instance around 90%, there are regions where with increasing WR, the energy consumption is not changing. These variations are due to the (in our view, unfortunate) choice to use Eq. (1) to define salt rejection in these RO calculations. Instead, Eq. (2) is rightfully the more common choice in literature, and using this definition of salt rejection, as we do in Fig. 1C, does not lead to the peculiar features shown in Fig. 1A, B. We use this definition of salt rejection by Eq. (2) in Fig. 1C, and here we obtain the more logical result that increasing water recovery always leads to higher, not lower, energy use. This use of Eq. (2) (Fig. 1C) to define salt rejection is the common choice in the desalination literature, and the authors of Ref. [1] also use Eq. (2) to describe salt rejection for their CDI calculations. We like to stress that comparing RO and CDI for the same water recovery, and purportedly the same salt rejection, but using Eq. (1) for RO and Eq. (2) for CDI can lead to large errors of judgement. For instance, for RO, comparing the calculation results of Fig. 1B and C, if we take a point of WR = 0.9 and R_{salt} = 0.9, we can observe a difference in predicted energy use of around a factor of 3.5, from ~0.14 kWh/m^3 using Eq. (1) (Fig. 1B) to ~0.45 kWh/m^3 using Eq. (2) (Fig. 2C). The error is that two situations are compared that are not comparable. Actually, at WR = 0.9, a salt rejection of $R_{salt,F}$ = 0.9 according to Eq. (2) (Fig. 1C) corresponds to a salt rejection of $R_{salt,B}$ = 0.989 according to Eq. (1) (as used in Fig. 1B). Thus, in a technology comparison where the numerical values of $R_{salt,B}$ and $R_{salt,F}$ are set equal (as well as the numerical value of WR), the technology that is analyzed using $R_{salt,B}$ is credited with a much lower energy use than would the other technology which is analyzed using $R_{salt,F}$ (when the numerical values of $R_{salt,B}$ and $R_{salt,F}$ are set equal). This difference, or error, is very large, especially at large WR and salt rejection, from a factor of exactly 2 at WR = 0.6 and R_{salt} = 0.6, to a value of 3.5 at

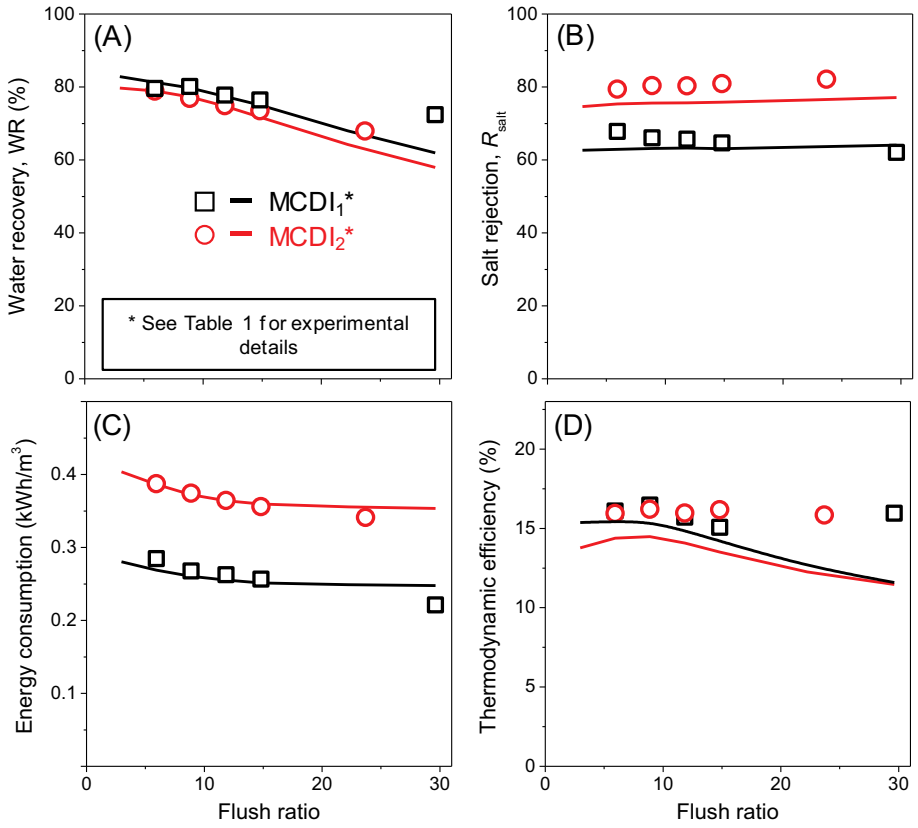

Fig. 3. Comparison of theory (lines) and data (symbols) for MCDI operation. (A) Water recovery, (B) salt rejection, (C) energy consumption assuming 100% energy recovery, and (D) thermodynamic efficiency, all as function of the flush ratio, FR (Eq. (4)), for a charging current density of 18.5 ($MCDI_1$) and of 22.0 A/m^2 ($MCDI_2$).

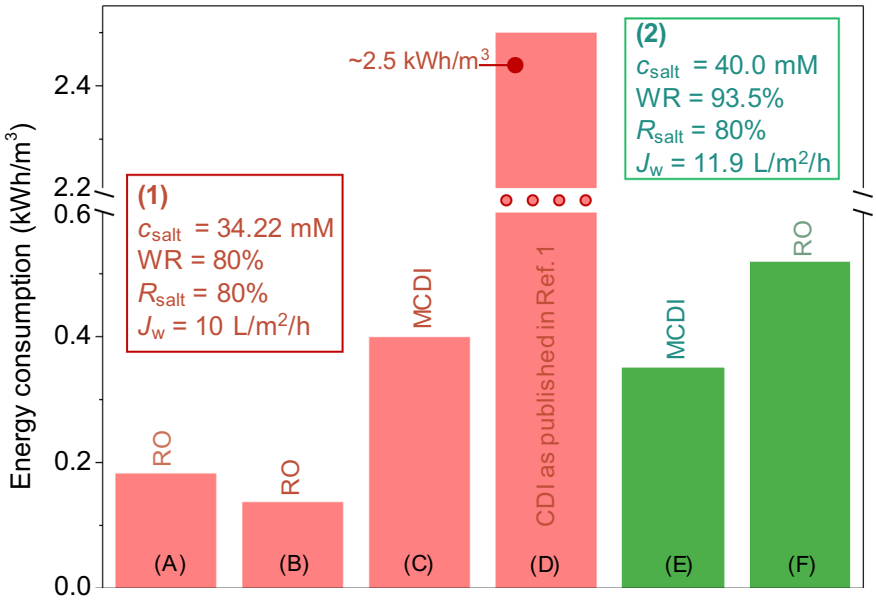

Fig. 4. Comparison of the calculated energy consumption of MCDI and RO using the salt rejection defined in Eq. (2). (A) Energy consumption of RO with an efficiency of the high-pressure pump, η_P, and of the energy recovery device, η_{ERD}, of 80% and (B) of 100%. (C) Energy consumption of MCDI based on parameters described in Table 1, whereas (D) is the CDI energy consumption reported by Qin et al. in Ref. [1]. (E) Energy consumption of an improved MCDI cell, see Table 1, operated with a higher water recovery (WR), compared with the energy consumption of RO (F) for the same desalination objective, and with η_P and η_{ERD} = 100%. All red bars are calculated at WR = 80%, R_{salt} = 80%, J_w = 10.0 L/m^2/h and feed salinity of 34.22 mM (2 g/L). The two green bars are calculated at WR = 93.5%, R_{salt} = 80%, J_w = 11.9 L/m^2/h and a feed salinity of 40 mM.

WR = 0.9, and R_{salt} = 0.9 and even higher values at higher WR. Thus, it is important to use the same definition of R_{salt} when comparing different methods or technologies. In this work we consistently use $R_{salt,F}$ given by Eq. (2).

4.2. Desalination results with intermittent flow operation

In the present work, we analyze the energy consumption of desalination by MCDI using a novel operational mode, the so-called intermittent flow mode, which was introduced by Ramachandran et al. [43]. Fig. 2 shows the current density, cell voltage and effluent concentration as function of time of our experiments described in Section 2 and Table 1. Compared to conventional CDI operation, we operate the cell with a low flow rate and a high current, resulting in a high salt rejection. Furthermore, we observe that the salt concentration of the flush-out water, or the brine, is high compared to conventional modes of operation used in CDI (see Fig. 2B, very right hand side). Fig. 2C shows the salt concentration in the electrodes and flow channel, and

shows very large concentration differences between the salt concentration in the electrodes and in the flow channel.

Fig. 3 shows data and theory of the desalination performance of MCDI as function of the flush ratio, FR, which is defined as the water volume pumped during flush-out period ($\Phi_{flo} \cdot t_{flo}$) divided by the open volume of the spacer material, and is given by

$$FR = \frac{\Phi_{flo} \cdot t_{flo}}{p_{sp} \cdot L_{sp} \cdot A_{cell}}. \quad (4)$$

We observe a good agreement between theory and data. With increasing flush ratio, both the water recovery and energy consumption decrease, but the salt rejection remains constant. For the same desalination objective (equal water recovery, salt rejection and salt concentration in the feed water), we find that the energy consumption of RO is lower than of MCDI. For a flush ratio of 8.9, RO requires ~0.163 kWh/m^3 to reach the same desalination objective as $MCDI_1$, and 0.200 kWh/m^3 for $MCDI_2$. We also find that, in intermittent flow operation, the water recovery can be increased from 0.5 to 0.76–0.80 without increasing the energy input (not reported in Fig. 3). We expect that the energy consumption can be further decreased. To optimize the performance and decrease the energy consumption, procedures described in Ref. [48] and Ref. [28] can be followed.

Finally, we compare the energy consumption of MCDI and RO for a feed water concentration of 34.22 mM (2 g/L), which matches with the concentration used in Ref. [1]. We consider a salt rejection of 80%, a water recovery of 80%, and a total flux of desalinated water of 10 L/m^2/h. In our analysis we consider that the efficiencies of the high-pressure pump, η_P, and of the energy recovery device, η_{ERD}, were both 80%, and we define R_{salt} according to Eq. (2). We also provide calculation results for the case when η_P and η_{ERD} are both 100%. Furthermore, we show the energy consumption for CDI as calculated by Ref. [1]. Fig. 4 shows that the energy consumption of MCDI is approximately two or three times higher than of RO, depending on which values for η_P and η_{ERD} are used. Clearly, the energy consumption of MCDI is much lower than the value of 2.5 kWh/m^3 reported for the same separation conditions by Qin et al. [1]. We also show that, if we increase the electrode thickness from 250 to 350 μm, and if we use electrode materials with a higher Stern layer capacity, we can prolong the desalination step, and increase the current density during charging as well. As one has to switch less frequently between desalination and regeneration, the water recovery can be increased to 93.5%, without an extra energy penalty. For these separation conditions, with high values for water recovery, the energy consumption of RO is higher than of MCDI. Interestingly, Ref. [1] for the same separation objective reports CDI energy consumption of ~4.0 kWh/m^3.

For the MCDI calculations, we can separate the energy into several parts: the energy consumption due to I) electronic resistances in cables and current collectors, the EER, II) ionic resistances in the electrodes, III) ionic resistances in the membranes, IV) Donnan potentials at the membrane interfaces, and V) the energy stored in the EDLs (Donnan and Stern layer). As discussed by Wang et al. [26], for MCDI with 100% energy recovery, and with ideal membranes, the energy stored in the EDLs (Donnan and Stern), can be completely recovered during discharge.

In our MCDI energy consumption analysis we used Eqs. (4.1)–(4.5) and (8.1)–(8.2) in Ref. [49], and we assumed, during regeneration, that 100% of the energy stored in the EDLs can be recovered. We find that the total energy consumption of an MCDI cycle in Fig. 4 is 0.4 kWh/m^3 desalinated water, and that 1% of the total energy is consumed due to ionic resistances in the electrodes, 6% is consumed due to ionic resistances in the membranes, 14% due to ionic resistances in the spacer channel, 17% due to electronic resistances in cables and current collectors, and 62% due to the Donnan potentials at the membrane interfaces.

5. Conclusions

In this work, we showed that CDI technology with membranes can achieve high values for water recovery, salt rejection and low values for energy consumption. We showed that, for separations with a water recovery close to 95%, the energy consumption of MCDI can be lower than that of Reverse Osmosis (RO), for which values of energy consumption are based on a system-scale model presented in Ref. [1]. This high water recovery is possible when electrodes with higher capacity and membranes with higher fixed charge density are used. Furthermore we showed that, in order to fairly compare desalination technologies, the same metric definitions must be used for the technologies subject to comparison, and that disparate definitions for salt rejection used in Ref. [1] do not allow for a fair comparison. Therefore, the results in the present work vary greatly from the results reported in Ref. [1]. The results reported in this work aim to facilitate an optimized operation of the CDI technology and contribute to a fair comparison between CDI and other desalination technologies, which is controversial at this moment.

CRediT authorship contribution statement

S. Porada:Investigation, Writing - original draft, Writing - review & editing.**Li Zhang**:Conceptualization, Writing - original draft, Writing - review & editing.**J.E. Dykstra**:Conceptualization, Writing - original draft, Writing - review & editing.

Declaration of competing interest

The authors declare that they have no known competing financial interests or personal relationships that could have appeared to influence the work reported in this paper.

Acknowledgement

This work was performed in the cooperation framework of Wetsus, European Centre of Excellence for Sustainable Water Technology (www.wetsus.eu). Wetsus is co-funded by the Dutch Ministry of Economic Affairs and Climate Policy, the Northern Netherlands Provinces, and the Province of Fryslân. This work is part of the Veni research programme with project number 15071, which is partly financed by the Dutch Research Council (NWO). The authors like to thank the participants of the research theme Capacitive Deionization for fruitful discussions and financial support.

References

[1] M. Qin, A. Deshmukh, R. Epsztein, S.K. Patel, O.M. Owoseni, W.S. Walker, M. Elimelech, Comparison of energy consumption in desalination by capacitive deionization and reverse osmosis, Desalination 455 (2019) 100–114, https://doi.org/10.1016/j.desal.2019.01.003.

[2] W. Shi, X. Zhou, J. Li, E.R. Meshot, A.D. Taylor, S. Hu, J.H. Kim, M. Elimelech, D.L. Plata, High-performance capacitive deionization via manganese oxide-coated, vertically aligned carbon nanotubes, Environ. Sci. Technol. Lett. 5 (2018) 692–700, https://doi.org/10.1021/acs.estlett.8b00397.

[3] M.E. Suss, S. Porada, X. Sun, P.M. Biesheuvel, J. Yoon, V. Presser, Water desalination via capacitive deionization: what is it and what can we expect from it? Energy Environ. Sci. 8 (2015) 2296–2319, https://doi.org/10.1039/C5EE00519A.

[4] S. Il Jeon, J. Lee, K. Jo, C. Kim, C. Lee, J. Yoon, Novel reuse strategy in flow-electrode capacitive deionization with switch cycle operation to enhance desalination performance, Environ. Sci. Technol. Lett. 6 (2019) 739–744, https://doi.org/10.1021/acs.estlett.9b00541.

[5] A.C. Arulrajan, D.L. Ramasamy, M. Sillanpää, A. van der Wal, P.M. Biesheuvel, S. Porada, J.E. Dykstra, Exceptional water desalination performance with anion-selective electrodes, Adv. Mater. 31 (2019) 1806937, , https://doi.org/10.1002/adma.201806937.

[6] Y. Salamat, C.H. Hidrovo, Significance of the micropores electro-sorption resistance in capacitive deionization systems, Water Res. 169 (2020) 115286, , https://doi.org/10.1016/j.watres.2019.115286.

[7] J. Ma, Y. Cheng, L. Wang, X. Dai, F. Yu, Free-standing Ti3C2Tx MXene film as binder-free electrode in capacitive deionization with an ultrahigh desalination

capacity, Chem. Eng. J. 384 (2020) 123329, , https://doi.org/10.1016/j.cej.2019.123329.
[8] W. Peng, W. Wang, G. Han, Y. Huang, Y. Zhang, Fabrication of 3D flower-like MoS2/graphene composite as high-performance electrode for capacitive deionization, Desalination 473 (2020) 114191, , https://doi.org/10.1016/j.desal.2019.114191.
[9] J. Han, T. Yan, J. Shen, L. Shi, J. Zhang, D. Zhang, Capacitive deionization of saline water by using MoS2-graphene hybrid electrodes with high volumetric adsorption capacity, Environ. Sci. Technol. 53 (2019) 12668–12676, https://doi.org/10.1021/acs.est.9b04274.
[10] T. Yan, J. Liu, H. Lei, L. Shi, Z. An, H.S. Park, D. Zhang, Capacitive deionization of saline water using sandwich-like nitrogen-doped graphene composites via a self-assembling strategy, Environ. Sci. Nano. 5 (2018) 2722–2730, https://doi.org/10.1039/C8EN00629F.
[11] P.M. Biesheuvel, R. Zhao, S. Porada, A. van der Wal, Theory of membrane capacitive deionization including the effect of the electrode pore space, J. Colloid Interface Sci. 360 (2011) 239–248, https://doi.org/10.1016/j.jcis.2011.04.049.
[12] J.B. Lee, K.K. Park, H.M. Eum, C.W. Lee, Desalination of a thermal power plant wastewater by membrane capacitive deionization, Desalination 196 (2006) 125–134, https://doi.org/10.1016/j.desal.2006.01.011.
[13] S. Porada, R. Zhao, A. van der Wal, V. Presser, P.M. Biesheuvel, Review on the science and technology of water desalination by capacitive deionization, Prog. Mater. Sci. 58 (2013) 1388–1442, https://doi.org/10.1016/j.pmatsci.2013.03.005.
[14] J. Choi, P. Dorji, H.K. Shon, S. Hong, Applications of capacitive deionization: desalination, softening, selective removal, and energy efficiency, Desalination 449 (2019) 118–130, https://doi.org/10.1016/j.desal.2018.10.013.
[15] X. Zhang, K. Zuo, X. Zhang, C. Zhang, P. Liang, Selective ion separation by capacitive deionization (CDI) based technologies: a state-of-the-art review, Environ. Sci. Water Res. Technol. (2020) 243–257, https://doi.org/10.1039/C9EW00835G.
[16] S.A. Hawks, M.R. Cerón, D.I. Oyarzun, T.A. Pham, C. Zhan, C.K. Loeb, D. Mew, A. Deinhart, B.C. Wood, J.G. Santiago, M. Stadermann, P.G. Campbell, Using ultramicroporous carbon for the selective removal of nitrate with capacitive deionization, Environ. Sci. Technol. 53 (2019) 10863–10870, https://doi.org/10.1021/acs.est.9b01374.
[17] T.M. Mubita, J.E. Dykstra, P.M. Biesheuvel, A. van der Wal, S. Porada, Selective adsorption of nitrate over chloride in microporous carbons, Water Res. 164 (2019) 114885, , https://doi.org/10.1016/j.watres.2019.114885.
[18] E.N. Guyes, T. Malka, M.E. Suss, Enhancing the ion-size-based selectivity of capacitive deionization electrodes, Environ. Sci. Technol. 53 (2019) 8447–8454, https://doi.org/10.1021/acs.est.8b06954.
[19] D.I. Oyarzun, A. Hemmatifar, J.W. Palko, M. Stadermann, J.G. Santiago, Ion selectivity in capacitive deionization with functionalized electrode: theory and experimental validation, Water Res. X. 1 (2018) 100008, , https://doi.org/10.1016/j.wroa.2018.100008.
[20] L. Wang, S. Lin, Mechanism of selective ion removal in membrane capacitive deionization for water softening, Environ. Sci. Technol. 53 (2019) 5797–5804, https://doi.org/10.1021/acs.est.9b00655.
[21] P. Nativ, O. Lahav, Y. Gendel, Separation of divalent and monovalent ions using flow-electrode capacitive deionization with nanofiltration membranes, Desalination 425 (2018) 123–129, https://doi.org/10.1016/j.desal.2017.10.026.
[22] W. Tang, P. Kovalsky, D. He, T.D. Waite, Fluoride and nitrate removal from brackish groundwaters by batch-mode capacitive deionization, Water Res. 84 (2015) 342–349, https://doi.org/10.1016/j.watres.2015.08.012.
[23] M.E. Suss, Size-based ion selectivity of micropore electric double layers in capacitive deionization electrodes, J. Electrochem. Soc. 164 (2017) E270–E275, https://doi.org/10.1149/2.1201709jes.
[24] Y. Qu, T.F. Baumann, J.G. Santiago, M. Stadermann, Characterization of resistances of a capacitive deionization system, Environ. Sci. Technol. 49 (2015) 9699–9706, https://doi.org/10.1021/acs.est.5b02542.
[25] J.E. Dykstra, R. Zhao, P.M. Biesheuvel, A. van der Wal, Resistance identification and rational process design in capacitive deionization, Water Res. 88 (2016) 358–370, https://doi.org/10.1016/j.watres.2015.10.006.
[26] L. Wang, J.E. Dykstra, S. Lin, Energy efficiency of capacitive deionization, Environ. Sci. Technol. 53 (2019) 3366–3378, https://doi.org/10.1021/acs.est.8b04858.
[27] A. Hemmatifar, J.W. Palko, M. Stadermann, J.G. Santiago, Energy breakdown in capacitive deionization, Water Res. 104 (2016) 303–311, https://doi.org/10.1016/j.watres.2016.08.020.
[28] J.E. Dykstra, S. Porada, A. van der Wal, P.M. Biesheuvel, Energy consumption in capacitive deionization – constant current versus constant voltage operation, Water Res. 143 (2018) 367–375, https://doi.org/10.1016/j.watres.2018.06.034.
[29] Y. Qu, P.G. Campbell, L. Gu, J.M. Knipe, E. Dzenitis, J.G. Santiago, M. Stadermann, Energy consumption analysis of constant voltage and constant current operations in capacitive deionization, Desalination 400 (2016) 18–24, https://doi.org/10.1016/j.desal.2016.09.014.
[30] S. Porada, L. Borchardt, M. Oschatz, M. Bryjak, J.S. Atchison, K.J. Keesman, S. Kaskel, P.M. Biesheuvel, V. Presser, Direct prediction of the desalination performance of porous carbon electrodes for capacitive deionization, Energy Environ. Sci. 6 (2013) 3700, https://doi.org/10.1039/c3ee42209g.
[31] R. Zhao, M. van Soestbergen, H.H.M. Rijnaarts, A. van der Wal, M.Z. Bazant, P.M. Biesheuvel, Time-dependent ion selectivity in capacitive charging of porous electrodes, J. Colloid Interface Sci. 384 (2012) 38–44, https://doi.org/10.1016/j.jcis.2012.06.022.
[32] J.E. Dykstra, K.J. Keesman, P.M. Biesheuvel, A. van der Wal, Theory of pH changes in water desalination by capacitive deionization, Water Res. 119 (2017) 178–186, https://doi.org/10.1016/j.watres.2017.04.039.
[33] P.M. Biesheuvel, S. Porada, M. Levi, M.Z. Bazant, Attractive forces in microporous carbon electrodes for capacitive deionization, J. Solid State Electrochem. 18 (2014) 1365–1376, https://doi.org/10.1007/s10008-014-2383-5.
[34] T. Kim, J.E. Dykstra, S. Porada, A. van der Wal, J. Yoon, P.M. Biesheuvel, Enhanced charge efficiency and reduced energy use in capacitive deionization by increasing the discharge voltage, J. Colloid Interface Sci. 446 (2015) 317–326, https://doi.org/10.1016/j.jcis.2014.08.041.
[35] J. Ma, C. He, D. He, C. Zhang, T.D. Waite, Analysis of capacitive and electrodialytic contributions to water desalination by flow-electrode CDI, Water Res. 144 (2018) 296–303, https://doi.org/10.1016/j.watres.2018.07.049.
[36] P.M. Biesheuvel, H.V.M. Hamelers, M.E. Suss, Theory of water desalination by porous electrodes with immobile chemical charge, Colloids Interface Sci. Commun. 9 (2015) 1–5, https://doi.org/10.1016/j.colcom.2015.12.001.
[37] X. Gao, S. Porada, A. Omosebi, K.L. Liu, P.M. Biesheuvel, J. Landon, Complementary surface charge for enhanced capacitive deionization, Water Res. 92 (2016) 275–282, https://doi.org/10.1016/j.watres.2016.01.048.
[38] E. Jones, M. Qadir, M.T.H. van Vliet, V. Smakhtin, S. Kang, The state of desalination and brine production: a global outlook, Sci. Total Environ. 657 (2019) 1343–1356, https://doi.org/10.1016/j.scitotenv.2018.12.076.
[39] R. Zhao, S. Porada, P.M. Biesheuvel, A. van der Wal, Energy consumption in membrane capacitive deionization for different water recoveries and flow rates, and comparison with reverse osmosis, Desalination 330 (2013) 35–41, https://doi.org/10.1016/j.desal.2013.08.017.
[40] S.A. Hawks, A. Ramachandran, S. Porada, P.G. Campbell, M.E. Suss, P.M. Biesheuvel, J.G. Santiago, M. Stadermann, Performance metrics for the objective assessment of capacitive deionization systems, Water Res. 152 (2019) 126–137, https://doi.org/10.1016/j.watres.2018.10.074.
[41] B.R. Sutherland, Arid forecasts for alternative energy-efficient desalination, Joule 3 (2019) 1410–1411, https://doi.org/10.1016/j.joule.2019.05.025.
[42] A. Ramachandran, D.I. Oyarzun, S.A. Hawks, P.G. Campbell, M. Stadermann, J.G. Santiago, Comments on “Comparison of energy consumption in desalination by capacitive deionization and reverse osmosis”, Desalination 461 (2019) 30–36, https://doi.org/10.1016/j.desal.2019.03.010.
[43] A. Ramachandran, D.I. Oyarzun, S.A. Hawks, M. Stadermann, J.G. Santiago, High water recovery and improved thermodynamic efficiency for capacitive deionization using variable flowrate operation, Water Res. 155 (2019) 76–85, https://doi.org/10.1016/j.watres.2019.02.007.
[44] S. Porada, M. Bryjak, A. van der Wal, P.M. Biesheuvel, Effect of electrode thickness variation on operation of capacitive deionization, Electrochim. Acta 75 (2012), https://doi.org/10.1016/j.electacta.2012.04.083.
[45] L.F. Greenlee, D.F. Lawler, B.D. Freeman, B. Marrot, P. Moulin, Reverse osmosis desalination: water sources, technology, and today’s challenges, Water Res. 43 (2009) 2317–2348, https://doi.org/10.1016/j.watres.2009.03.010.
[46] B.M. Ganesh, A.M. Isloor, A.F. Ismail, Enhanced hydrophilicity and salt rejection study of graphene oxide-polysulfone mixed matrix membrane, Desalination 313 (2013) 199–207, https://doi.org/10.1016/j.desal.2012.11.037.
[47] H.T. El-Dessouky, H.M. Ettouney, Reverse osmosis, in: H.T. El-Dessouky, H.M. Ettouney (Eds.), Fundam. Salt Water Desalin, Elsevier, Amsterdam, 2002, pp. 409–437, , https://doi.org/10.1016/B978-044450810-2/50009-9.
[48] A. Ramachandran, S.A. Hawks, M. Stadermann, J.G. Santiago, Frequency analysis and resonant operation for efficient capacitive deionization, Water Res. 144 (2018) 581–591, https://doi.org/10.1016/j.watres.2018.07.066.
[49] J.E. Dykstra, Desalination with Porous Electrodes, PhD thesis, Wageningen University, 2018.